BIOFILM GROWTH IN DRINKING WATER SYSTEMS UNDER STAGNANT CONDITIONS

Erifyli Tsagkari* and William T. Sloan

School of Engineering, College of Science and Engineering, University of Glasgow,

G12 8LT, United Kingdom

*Corresponding author: e-mail: Erifyli.Tsagkari@glasgow.ac.uk, tel: +447833637863

Abstract

Safe drinking water is essential for human health and its provision in a changing climate is a global pressing problem. Research communities, governments and drinking water supplying companies are working on improving the quality of drinking water and reducing its cost. Microorganisms colonise the inner surfaces of pipes and form biofilms. In drinking water systems biofilms are problematic as they cause loss of disinfectants, harbour pathogens and affect the aesthetics of drinking water. From the engineering perspective, that leads to corrosion of the pipe's material and reduced life of the existing infrastructure. Thus, it is imperative that we gain a deeper understanding of the growth of biofilms if we are to develop effective strategies for their removal or control.

In this study we focused on the growth of biofilms in drinking water under stagnant conditions, which often occur in parts of drinking water pipes. A bioreactor was used to simulate the service lines of drinking water systems. After 4 weeks, the thickness and density of the biofilms were characterised using gravimetric measurements, and their surface area was determined using fluorescence microscopy. Also, the concentration of cells and microcolonies both in the bulk water and on the reactor surfaces was determined using fluorescence microscopy. Finally, spatial statistics were used to describe the biofilm structures that were formed on the exposed surfaces of the reactor. It was revealed that even under stagnant and oligotrophic conditions, drinking water bacteria moved from the bulk water of the reactor and attached to the available surfaces forming a high number of microcolonies. Biofilms were able to grow on the exposed surfaces of the reactor forming characteristic structures consisting of dense cell clusters. Our results revealed that even under unfavourable conditions biofilms can grow within our drinking water systems.

Keywords

biofilms; drinking water; microscopy; reactor; stagnant

1. INTRODUCTION

Biofilms are found on virtually every wetted surface on earth. Even though the term "biofilm" may not form part of the popular lexicon, most people are familiar with biofilms in one way or another, in particular with those that can be seen by naked eye. The plaque on our teeth is a biofilm, the slime on our contact lenses, the bathroom walls or rotting food is also a biofilm. Similarly, the green of brown coating on rocks, pebbles or sand in a river is a biofilm [Hall-Stoodley et al., 2004]. A biofilm consists of a group of microorganisms, such as bacteria, fungi, viruses and protozoa,

which adhere to a surface and are usually housed in a matrix of extracellular polymeric substances (EPS). The EPS are biopolymers including polysaccharides, proteins, nucleic acids and lipids. In most biofilms, the microorganisms may account for less than 10% of the total biofilm dry mass, whereas the EPS matrix may account for over 90% of that. The biofilm matrix has been characterised as a three-dimensional polymer network that interconnects and immobilises the cells that it consists of [Flemming and Wingender, 2010].

It is estimated that 99% of the total population of bacteria in the world are found in the form of a biofilm [Florjanic and Kristl, 2011]. One of the main reasons why bacteria opt for the biofilm, rather than the planktonic mode of life, is the protection that the biofilm offers to them. This might include protection against harsh conditions, such as nutrient deprivation, shear stresses, ultraviolet or acid exposure, metal toxicity, dehydration, salinity, antibiotics and other antimicrobial agents [Hall-Stoodley et al., 2004].

Biofilms can be very useful, especially in the field of bioremediation. Organisms may be used for contaminant removal and for the purification of industrial wastewater. In biofilm filtration systems, the filter medium presents a surface for the microbes to attach to and to feed on the organic material in the water being treated. Such water cleaning systems are biologically more stable and their disinfectant demand is lower than that of conventionally treated systems. Less microorganism induced contamination is likely to occur in water that passes through a biofilm based filter than there is in water that passes through another alternative treatment system [Campos et al., 2002].

On the other hand, biofilms can result in heavy costs for the cleaning and maintenance of the industrial and domestic pipes that they colonise. The environment in which people are mostly exposed to biofilms is the domestic environment [Garrett et al., 2008]. Although drinking water is closely monitored in the developed countries, waterborne disease outbreaks are still being reported. These outbreaks may be associated with pathogenic bacteria and viruses, and biofilms in the water pipe networks are known to create favourable conditions for their survival and growth. In addition, the detachment of biofilms from pipe walls is associated with changes in the water taste, odour and colour. The main challenge of drinking water industries is to deliver water that is microbiologically and chemically safe, aesthetically pleasing and adequate in quantity [Simões, 2012]. Thus, it is crucial to find ways of managing the biofilms that will inevitably form.

Visualising biofilm structures is complicated due to the presence of debris, corrosion products and mineral deposits, which provide new niches for bacteria to colonise [Batté et al., 2003]. Organic and inorganic particles can accumulate in low-flow areas or dead-ends of drinking water systems and enhance microbial activities by providing protection for bacteria against harsh conditions [Simões, 2012, Douterelo et al., 2013]. Biofilms are generally found to form very complex and heterogeneous structures [van Loodsdrecht et al., 1995]. Thicknesses that have been recorded for biofilms in drinking water systems range from a few tens of micrometres [Srinivasan et al., 2008] to a few hundreds of micrometres [Momba et al., 2000]. Biofilms may be formed on the surfaces of drinking water pipes within a few days or months and may reach a cell concentration of 10^7-10^9 cells/cm^2 [Manuel, 2007]. The vast majority of bacteria, estimated at 95% of the total cell population, are attached to the surfaces of the pipes, whereas only 5% are found in the water phase [Flemming et al., 2002].

In drinking water systems under high flow conditions, which are those that are mostly experienced, microorganisms are transported by eddies in the flow [Kumarasamy and Maharaj, 2015]. Under low flow conditions, the transport of bacteria from the bulk water to the exposed surfaces occurs due to Brownian diffusion, sedimentation and cell motility. Stagnant conditions occur regularly in drinking water systems (i.e. during overnight periods or near closed valves and flanges in the system) when the water consumption is low [Manuel et al., 2007]. It is suspected that the biofilm growth characteristics under stagnant conditions would be similar to those in laminar flow, where shear stresses are low and the transport of nutrients and oxygen is driven by diffusion. However, very little is known about biofilm growth under such conditions [Manuel et al., 2007, Liu et al., 2016].

Thus, in this study, the development of biofilms in drinking water was investigated under stagnant conditions after a 4-week period using a bioreactor. A 4-week period is considered a realistic time period of water stagnation in service lines [Zlatanović et al., 2017]. Also, the reactor, which was used, simulated the part of drinking water distribution systems, which is closer to the tap. The exact structure and composition of drinking water biofilms are still unclear and have not been described in detail yet due to difficulties in investigating such a small amount of biomass without disturbing it. Biofilms in drinking water systems are generally thin but these low thicknesses that can be reached are variable [Wimpenny et al., 2000]. Thus, the goal of this study was to investigate how biofilms were developed under oligotrophic conditions in stagnant water and to characterize them.

2. MATERIALS AND METHODS

2.1 Reactor conditions

Biofilms were grown in a jacketed rotating annular reactor (model 1320 LJ, BioSurface Technologies, US). This reactor presents various advantages such as simple sampling process. Also, the liquid phase of reactor is well mixed, which ensures that there is uniform distribution of bacteria in the bulk liquid [Characklis and Marshall, 1990]. The reactor held 20 new and sterile vertical polycarbonate slides (BST-503-PC) attached to its inner drum. The beveled edges of the slides were dropped into the beveled slots on the reactor inner cylinder and they were removed from it using a sterilized hook. The slides were placed in the inner cylinder in a symmetric way in order to avoid any imbalances. The polycarbonate material of the slides was chosen as one of the plastic materials, which are used in drinking water systems [Szabo et al., 2007, Garny et al., 2008]. The jacket of the reactor allowed the temperature to be maintained in the system via heated water from a bath circulator (Isotemp Bath Circulator, Fisher Scientific, UK). The temperature was chosen at 16^{o}C as the representative temperature of DWDS in the United Kingdom for spring and summer [Douterelo et al., 2013]. The reactor was covered with aluminium foil in order to achieve dark conditions for biofilm growth. The diameter of the pipe, which was simulated using this reactor, was at 30.3 mm. This pipe diameter corresponds to the extremities of drinking water systems where the service lines start [Hall et al., 2009]. The conditions in service lines are generally characterised by longer residence times, higher stagnation periods, reduced flow rates and higher temperatures compared to those in the mains [Zheng et al., 2015].

The medium that the reactor was filled with consisted of 150 ml of nutrient medium and 850 ml of drinking water that was sampled from a domestic tap in Glasgow. The concentrations for mineral salts of the reactor medium were: ammonium sulphate (1.2 mg/l), ammonium chloride (0.9 mg/l), magnesium sulphate heptahydrate (0.3 mg/l), manganese chloride tetrahydrate (0.003 mg/l), copper sulphate pentahydrate (0.002 mg/l), cobalt sulphate heptahydrate (0.001 mg/l), sodium molybdate dehydrate (0.001 mg/l), zinc sulphate heptahydrate (0.01 mg/l), and boric acid (0.75 mg/l) (Milferstedt et al., 2006), and the concentration for glucose of the reactor medium was 1.5 mg/l. These concentrations kept the bulk water conditions in the reactor oligotrophic (Batté et al., 2003). The total organic carbon (TOC) in the bulk water of reactor was determined using a TOC-L analyser (SHIMADZU, Japan) as the difference between the total carbon and the total inorganic carbon. To calculate the TOC 3 samples of 10 ml each were used. The TOC was measured at the onset of the experiment and after 4 weeks. Finally, the concentration of total chlorine of the drinking water, which was sampled from the tap, was measured immediately after its sampling and after 4 weeks. The USEPA DPD Method 8167 [Chamberlain and Adams, 2006] was followed to measure the chlorine concentration using the DR 900 Hach colorimeter (Colorado, US). The measurements were performed for 3 samples of 10 ml each.

2.2 Cells and microcolonies measurements

To calculate the concentration of cells in the bulk water of reactor at the onset of the experiment 3 samples of 5 ml each were used. These samples were filtered through 47 mm Whatman® 0.2 μm membrane filters (Sigma-Aldrich, Irvine, UK) after they were fixed with 0.5 ml of 2% formaldehyde [Kepner and Pratt, 1994]. The membrane filters were then covered with 1 ml of 0.1% Triton X-100 solution in order to evenly disperse the cells. The cells on the membrane filters were then stained with 1 ml of 10 μg/ml (4′,6-diamidino-2-phenylindole) DAPI for 20 minutes in the dark and visualised using fluorescence microscopy (Olympus IX71, Japan) with the oil immersion UPlanFLN objective lens (100X magnification/1.30 numerical aperture). More than 30 images per membrane filter were obtained. The concentration of cells was calculated from [Brunk et al., 1979]:

$$\frac{\text{cells}}{\text{ml}} = \frac{\left(\frac{\Sigma x}{\text{n}} \pm s\right) \text{A}_{\text{memb}} \text{d}}{\text{A}_{\text{field}} \text{V}_{\text{filt}}} \quad (1)$$

where $\Sigma x/\text{n}$ is the mean number, s is the standard deviation, A_{memb} is the surface area of the membrane filter, d is the dilution factor, A_{field} is the surface area of the microscope field and V_{filt} is the volume of the liquid sample filtered. The same procedure was used to calculate the concentration of microcolonies in the bulk water of reactor but without using the Triton solution and by using the objective lens with 10X magnification/0.30 numerical aperture instead of the one with 100X magnification/1.30 numerical aperture. The microcolonies visualised had a diameter of approximately 10 μm and consisted of approximately 10 cells.

To calculate the concentration of cells on the reactor slides after the 4 weeks, 3 slides were removed from the reactor. The biomaterial attached to the reactor slides was gently scraped from the slides and diluted in 5 ml distilled water. Then, the 5 ml samples were fixed with 0.5 ml of 2% formaldehyde [Kepner and Pratt, 1994] and filtered on Whatman® 0.2 μm membrane filters. The same procedure described above was followed. The concentration of cells was calculated from [Brunk et al., 1979]:

$$\frac{\text{cells}}{\text{cm}^2} = \frac{\left(\frac{\Sigma x}{\text{n}} \pm s\right) \text{A}_{\text{memb}} \text{d} \text{V}_{\text{susp}}}{\text{A}_{\text{field}} \text{V}_{\text{filt}} \text{A}_{\text{biof}}} \quad (2)$$

where V_{susp} is the total suspension volume and A_{biof} is the area from which the biomaterial was scraped. The same procedure was used to calculate the concentration of microcolonies on the reactor slides. The microcolonies were similar to those described above.

2.3 Biofilm measurements

To calculate the biofilm thickness and density 3 slides were removed from the reactor. Gravimetric measurements were used to characterise the thickness and density of the biofilms attached to the slides [Staudt et al., 2004]. In brief, after the slides were removed from the reactor they were drained for 5 minutes at a vertical position and then they were weighed for the determination of the wet mass. Then, the slides were dried for 24 hours at 65^{o}C in an oven and weighed again. After that, the dried biofilm was washed off the slides with distilled water and laboratory tissues. The clean slides were dried again for 24 hours at 65^{o}C and then weighed again. The dry mass was determined by the weight difference of the slides with and without the dried biofilm. The biofilm thickness, L_F, was determined by:

$$L_F = \frac{m_{WF}}{\rho_{\text{WF}} \text{A}_{\text{F}}} \quad (3)$$

and the volumetric biofilm density, ρ_F, was determined by:

$$\rho_F = \frac{m_{DF}}{\left(\frac{m_{WF}}{\rho_{WF}}\right)} \quad (4)$$

where m_{WF} and m_{DF} are the wet and dry mass of the biofilm respectively. Also, ρ_{WF} is the density of biofilm, for which there is the assumption that it is equal to that of water at 16^{o}C at 998.946 kg/m^3. Finally, A_F is the surface area of the slide. The areal biofilm density was finally calculated as the product of the biofilm thickness and the volumetric biofilm density.

To visualise the biofilm structures on the reactor slides after the 4 weeks, 3 slides were removed from the reactor. The biofilms on the reactor slides were firstly fixed with 0.5 ml of 4% paraformaldehyde [Chao and Zhang, 2011]. The samples were covered with 1 ml of 10 μg/ml DAPI for 20 minutes in the dark. Biofilm structures were visualised using the objective lens with 100X magnification/1.30 numerical aperture. The surface area of biofilms on the reactor surfaces was then calculated in Matlab by processing more than 30 images obtained from fluorescence microscopy. The original images were firstly converted to gray-scale images using the Matlab command called "rgb2gray" and then to binary images using the Matlab command called "im2bw" in order to separate the biomaterial from the background of the image. After the surface area of the biofilm was calculated, it was divided to the total surface area of the image in order to finally calculate the percentage of this surface area (%).

2.4 Spatial statistics

Textural entropy was used to characterise the biofilm structures. Entropy is used to describe the randomness of the components of a gray-scale image by comparing the intensity of the image pixels. The higher is the value of the entropy, the more heterogeneous is the biofilm. This means that more complex biofilm structures are demonstrated in the image. Entropy refers to the gray levels, which the individual pixels can adopt. In an 8-bit pixel image, for example, there are 256 such levels [Yang et al., 2000, Beyenal et al., 2004]. The entropy, E, is here defined:

$$E = -\sum p \log_2 p \quad (5)$$

where p is the pixel intensity associated with the gray level. Entropy was calculated using the Matlab function called "entropy". To calculate the entropy more than 30 images of the biofilm structures, obtained from fluorescence microscopy, were used.

The semi-variogram was used as another measure to characterise the spatial variance of biofilm structures within gray-scale images and quantify the spatial dependencies in the data sets. Its function relates the semi-variance of the data points to the distance that separates them. Large distance of the data points means more data pairs for the estimation of the semi-variance but less amount of detail in the semi-variogram. In other words, the semi-variogram is a way of graphically capturing the spatial variance of points on a landscape as a function of their distance. All combinations of points at a distance are collated and their variance is determined for all possible separation distances [Carr and de Miranda, 1998]. The semi-variogram was calculated using the Matlab function called "variogram.m".

The autocorrelation function (ACF) diagram was used as the last measure to characterise the biofilm structures. The ACF diagram is, in essence, a two-dimensional extension of the semi-variogram. It allows us to assess how the spatial autocorrelation changes with distance. It correlates pixel intensities within gray-scale images and detects the repetitive structures within the image under consideration by combining together all parts of it. The ACF diagram is a real-space image, so that its dimensions have the same meaning as in the original image. Interpretation of the ACF diagram can be understood by imagining the image to be printed on transparency and placed on top of itself but rotated by 180^{o}. By sliding the top image laterally in any direction, the degree of match with the underlying original image is measured by this function [Heilbronner and Barrett, 2014]. The ACF diagram was calculated using the Matlab function called "autocorr2d.m".

3. RESULTS AND DISCUSSION

3.1 Reactor medium, cells and microcolonies

The total chlorine of drinking water after it was sampled from the tap was found at 0.36 mg/l and after the 4 weeks it was found at 0 mg/l, as it was expected, since chlorine can decay through its interactions with the material of the slides or with the adhering on them biofilms [Brown et al., 2011]. Also, the TOC of reactor medium at the onset of the experiment was found at (1.95±0.3) mg/l and after the 4 weeks it was found at (0.74±0.1) mg/l. This showed that the TOC was decreased with time probably due to its consumption from the bacteria. The concentration of cells in the bulk water was found at $(5.1 \pm 0.5)*10^5$ cells/ml and the concentration of microcolonies in the bulk water was determined at $(3.6\pm0.2)*10^3$ microcolonies/ml at the onset of the experiment. This showed that cells were formed into microcolonies in the drinking water that was sampled from the tap rather than only being at their own state. The concentration of cells on the reactor slides was determined at $(1.9 \pm 0.3)*10^3$ cells/cm^2 (Figure 1a) after 4 weeks. This indicated that a quite high portion of the bacteria that were in the bulk water at the onset of the experiment were finally transferred to the reactor slides after the 4-week period. The concentration of microcolonies on the reactor slides after the 4-week period was found at $(2.6 \pm 0.7)*10^2$ microcolonies/cm^2 (Figure 1b). This showed again that a quite high portion of the cells formed microcolonies on the reactor slides after 4 weeks. A microcolony is a form of aggregate, which is the coming together of bacteria in the bulk water that might be transferred finally onto the available surfaces. Thus, it is considered to be an important precursor for the formation of biofilms [Sheng et al., 2010, Saur et al., 2017].

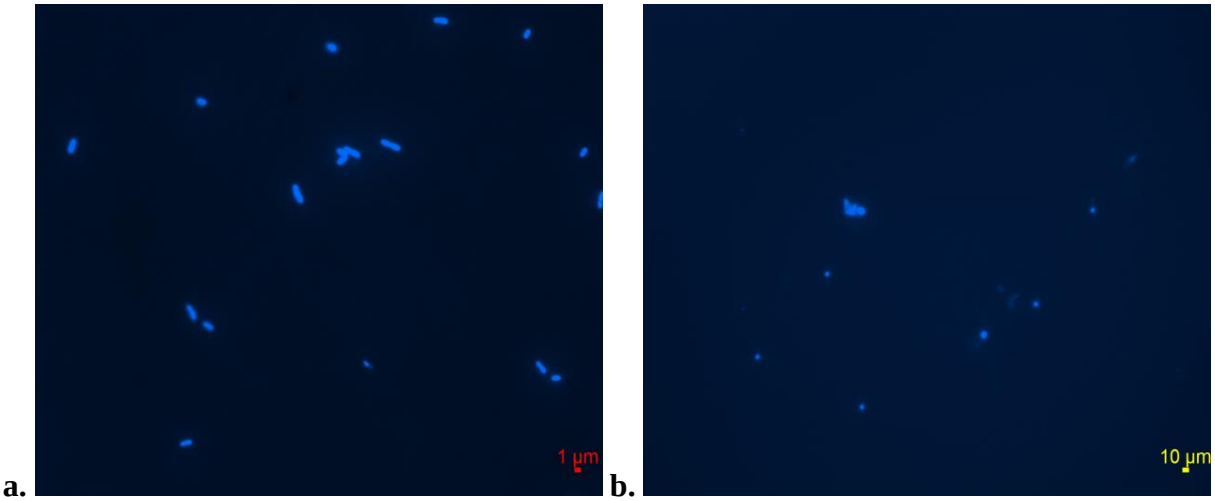

Figure 1

a) Cells of about 1 µm size attached to the reactor slides, b) microcolonies of about 10 µm size attached to the reactor slides as revealed by fluorescense microsocpy.

3.2 Biofilms

Under stagnant conditions, given that bacteria are not transported onto surfaces by flowing water, then one might expect gravity to have an effect; thus, the vertical slides of reactor to be less prone to cell colonisation. Also, the oligotrophic conditions implicate that there is not enough energy given to bacteria to come together to each other and form biofilms. Shear stress conditions have a number of effects on bacteria; they keep them in suspension and increase the probability of bacteria colliding by chance. They also enhance mass transfer processes, oxygen distribution within the bulk water of pipelines and any metabolic reactions between bacteria [Lee et al., 2002, Son et al., 2015]. Thus, it was surprising to find that biofilms did grow in drinking water under stagnant conditions and their percentage of surface area after 4 weeks was found at 19.2%. Also, after 4 weeks the thickness of biofilms was found at 119.54 µm and their density at 9 mg/cm^2. This validated that biofilms did form in drinking water under stagnant conditions. However, the thickness of the

biofilm was not high compared to the thicknesses that have been found using the same method under shear stress conditions [Horn et al., 2003, Staudt et al., 2004, Elenter et al., 2007].

3.3 Biofilm structures

Biofilms were found to form patchy structures consisting of rod-shaped bacteria (Figure 2) as revealed by fluorescence microscopy. The hazy part of biofilms in Figure 2 is probably the EPS of biofilms, which surrounded the cells. This patchy structure is also seen in laminar flow conditions where shear stresses are low [Stoodley et al., 1999a]. In turbulent flows biofilms tend to form much different structures such as filamentous structures that are also called streamers [Besemer et al., 2009]. However, streamers have been also identified in rare cases in laminar flow conditions [Rusconi et al., 2010]. Bacteria under low flow conditions tend to form clusters, which are microcolonies that consist of densely packed cells held together by EPS. Thus, the patchy structures consisting of cell clusters, which were identified here, were not a surprising result.

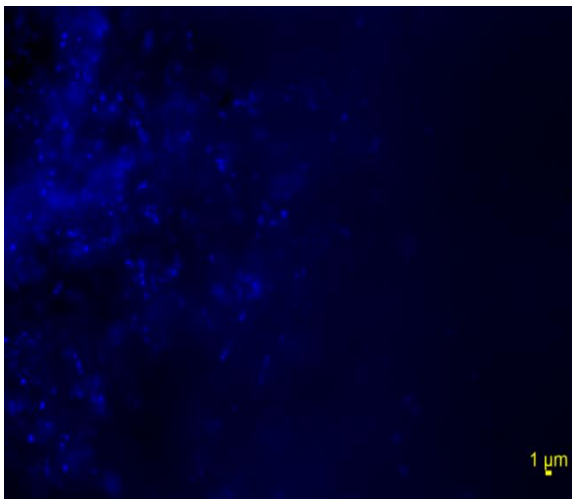

Figure 2

Biofilm structures stained with DAPI as revealed by fluorescence microscopy.

The entropy of biofilms was determined at 1.87. If all of the pixels of the image have the same value, or the image has no structures, or the image is composed of only white pixels or voids, the entropy of the image is 0 showing there is no gray scale variation in the pixels or heterogeneity. Increased numbers of structures in the image increase entropy due to increased gray level variability and heterogeneity in the image [Yang et al., 2000]. Thus, our measurements revealed that since entropy was not 0 or close to 0 this shows that characteristic biofilm structures were actually formed on the reactor surfaces.

The semi-variogram is here demonstrated (Figure 3a). An important part of a semi-variogram is the "origin", which represents the closest points of the diagram. Another important part of a semi-variogram is the "sill", which is the variogram upper bound that is equal to the variance of the data set and it also reflects the amount of variability. The sill is usually found at large distances where there is no gradient in the diagram [Cohen et al., 1990, Cressie, 1993]. The lag distance at which the semi-variogram reaches the sill value is the "range". In total, 12000 points were used for the calculation of the semi-variogram shown in Figure 3a. The gradient in the variance close to the origin was found to be shallow and linear. This indicated that values were co-located as the variance at short distance was found to be low. These measurements showed that the topography of the biofilm was now very heterogeneous, as it was expected for stagnant conditions [Stoodley et al., 1999b]. Finally, the range was found at about 70 μm and the sill was equal to almost 9.

The ACF diagram is here demonstrated as a contour plot (Figure 3b). The almost radially symmetric contours in autocorrelation do not suggest that there was only one spatially-correlated "lump" at the centre of the image. It is the average autocorrelation for all pixels on the image. In the ACF diagram, the central element provides a measure of the size and shape of the basic element that dominates the original image. The rest contour lines reflect the size and shape of the neighbourhood elements of the original image. Finally, the bar on the right side of the ACF diagrams provides a measure of the autocorrelation. The darker is the colour on the bar, the less is the autocorrelation value with its lowest value to be 0 and the highest one to be 1 [Russ, 2011]. In this diagram, the central element was found to be a circular feature, which size and shape corresponded to a cell. The rest contour lines, which were found to surround this main feature, were also circular and corresponded to a microcolony. These measurements suggest that radially symmetrical lumps were the prevalent topographical features, which could be associated with microcolonies. The contour plot in Figure 3b showed that cells align with themselves creating characteristic microcolonies, as it was also indicated in Figure 2.

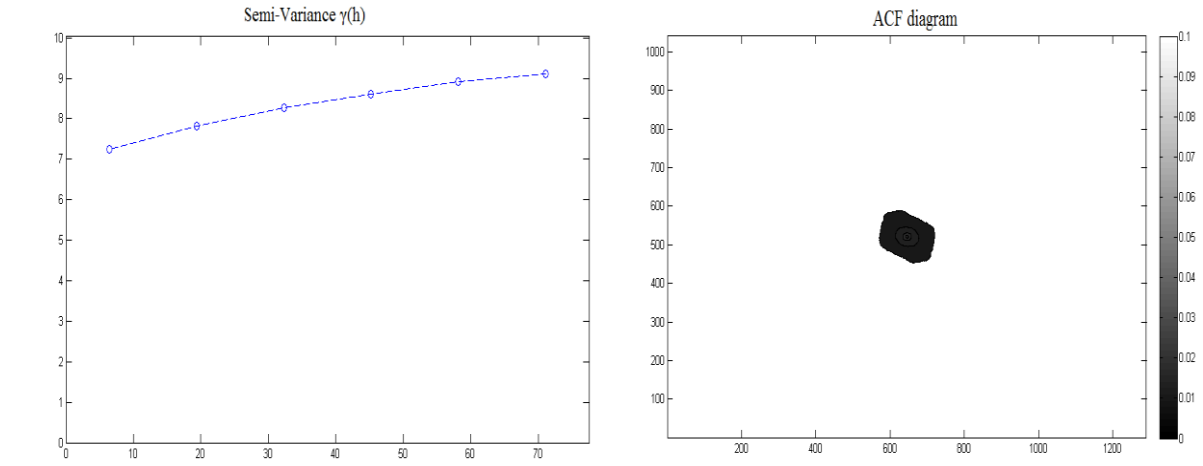

Figure 3

a) Semi-variogram; the vertical axis represents the semi-variance and the horizontal one represents the distance in μm, b) ACF diagram; the axes represent the size of the original image in pixels.

Overall, an annular reactor allowed us to grow biofilms in drinking water under stagnant conditions. Understanding the functionality and mechanisms of biofilms during the moderate (weeks) stages of their life will help in the consideration of future design of management strategies to control their growth in real drinking water systems. Our experiments suggest that biofilms were able to form in the reactor even under stagnant and oligotrophic conditions. However, these biofilms were not very thick and dense as it was revealed by gravimetric measurements. Fluorescence microscopy also revealed that biofilms were actually formed on the reactor surfaces creating characteristic patchy structures consisting of cell clusters. Finally, spatial statistics showed that the microcolonies were the most evident feature of the biofilm structures, which were not found to be complex, heterogeneous and irregular. Engineers should not overlook the biofilm-associated problems since a cursory understanding of the biology of the microorganisms that sit at the boundaries of our existing infrastructure will lead to an enhanced functionality of them.

REFERENCES

1. Batté, M., Appenzeller, B. M. R., Grandjean, D., Fass, S., Gauthier, V., Jorand, F., Mathieu, L., Boualam, M., Saby, S. and Block, J. C. (2003). 'Biofilms in drinking water distribution systems'. **Reviews in Environmental Science and Bio/Technology**, 2**,** pp. 147-168.

2. Besemer, K., Hodl, I., Singer, G. and Battin, T. J. (2009). 'Architectural differentiation reflects bacterial community structure in stream biofilms'. **Isme Journal**, 3**,** pp. 1318-1324.
3. Beyenal, H., Donovan, C., Lewandowski, Z. and Harkin, G. (2004). 'Three-dimensional biofilm structure quantification'. **J Microbiol Methods**, 59**,** pp. 395-413.
4. Brown, D., Bridgeman, J. and West, J. R. (2011). 'Predicting chlorine decay and THM formation in water supply systems'. **Reviews in Environmental Science and Bio-Technology**, 10**,** pp. 79-99.
5. Brunk, C. F., Jones, K. C. and James, T. W. (1979). 'Assay for Nanogram Quantities of DNA in Cellular Homogenates'. **Analytical Biochemistry**, 92**,** pp. 497-500.
6. Campos, L. C., Su, M. F. J., Graham, N. J. D. and Smith, S. R. (2002). 'Biomass development in slow sand filters'. **Water Res**, 36**,** pp. 4543-4551.
7. Carr, J. R. and de Miranda, F. P. (1998). 'The semivariogram in comparison to the co-occurrence matrix for classification of image texture'. **Ieee Transactions on Geoscience and Remote Sensing**, 36**,** pp. 1945-1952.
8. Chamberlain, E. and Adams, C. (2006). 'Oxidation of sulfonamides, macrolides, and carbadox with free chlorine and monochloramine'. **Water Res**, 40**,** pp. 2517-2526.
9. Chao, Y. Q. and Zhang, T. (2011). 'Optimization of fixation methods for observation of bacterial cell morphology and surface ultrastructures by atomic force microscopy'. **Appl Microbiol Biotechnol**, 92**,** pp. 381-392.
10. Characklis, W. G. and Marshall, K. C. 1990. '**Biofilms'**, New York: John Wiley and Sons.
11. Cohen, W. B., Spies, T. A. and Bradshaw, G. A. (1990). 'Semivariograms of Digital Imagery for Analysis of Conifer Canopy Structure '. **Remote Sens. Environ.**, 34**,** pp. 167-178.
12. Cressie, N. 1993. '**Statistics for spatial data, Wiley series in probability and mathematical statistics, Revised Edition'**, New York, Wiley.
13. Douterelo, I., Sharpe, R. L. and Boxall, J. B. (2013). 'Influence of hydraulic regimes on bacterial community structure and composition in an experimental drinking water distribution system'. **Water Res**, 47**,** pp. 503-16.
14. Elenter, D., Milferstedt, K., Zhang, W., Hausner, M. and Morgenroth, E. (2007). 'Influence of detachment on substrate removal and microbial ecology in a heterotrophic/autotrophic biofilm'. **Water Res**, 41**,** pp. 4657-4671.
15. Flemming, H. C., Percival, S. L. and Walker, J. T. (2002). 'Contamination potential of biofilms in water distribution systems'. **Innovations in Conventional and Advanced Water Treatment Processes**, 2**,** pp. 271-280.
16. Flemming, H. C. and Wingender, J. (2010). 'The biofilm matrix'. **Nature Reviews Microbiology**, 8**,** pp. 623-633.
17. Florjanic, M. and Kristl, J. (2011). 'The control of biofilm formation by hydrodynamics of purified water in industrial distribution system'. **International Journal of Pharmaceutics**, 405**,** pp. 16-22.
18. Garny, K., Horn, H. and Neu, T. R. (2008). 'Interaction between biofilm development, structure and detachment in rotating annular reactors'. **Bioprocess Biosyst Eng**, 31**,** pp. 619-629.
19. Garrett, T. R., Bhakoo, M. and Zhang, Z. (2008). 'Bacterial adhesion and biofilms on surfaces'. **Progress in Natural Science**, 18**,** pp. 1049-1056.
20. Hall-Stoodley, L., Costerton, J. W. and Stoodley, P. (2004). 'Bacterial biofilms: from the natural environment to infectious diseases'. **Nat Rev Microbiol**, 2**,** pp. 95-108.
21. Hall, J., Szabo, J., Panguluri, S. and Meiners, G. (2009). 'Distribution System Water Quality Monitoring: Sensor Technology Evaluation Methodology and Results' A Guide for Sensor Manufacturers and Water Utilities. Environmental Protection Agency (EPA), USA.
22. Heilbronner, R. and Barrett, S. (2014). '**Image Analysis in Earth Sciences**', Springer.

23. Horn, H., Reiff, H. and Morgenroth, E. (2003). 'Simulation of growth and detachment in biofilm systems under defined hydrodynamic conditions'. **Biotechnol Bioeng**, 81**,** pp. 607-617.
24. Kepner, R. L. and Pratt, J. R. (1994). 'Use of Fluorochromes for Direct Enumeration of Total Bacteria in Environmental-Samples - Past and Present'. **Microbiological Reviews**, 58**,** pp. 603-615.
25. Kumarasamy, M. V. and Maharaj, P. M. (2015). 'The Effect of Biofilm Growth on Wall Shear Stress in Drinking Water PVC Pipes'. **Polish Journal of Environmental Studies**, 24**,** pp. 2479-2483.
26. Lee, S. H., Lee, S. S. and Kim, C. W. (2002). 'Changes in the cell size of Brevundimonas diminuta using different growth agitation rates'. **PDA J Pharm Sci Technol**, 56**,** pp. 99-108.
27. Liu, S., Gunawan, C., Barraud, N., Rice, S. A., Harry, E. J. and Amal, R. (2016). 'Understanding, Monitoring, and Controlling Biofilm Growth in Drinking Water Distribution Systems'. **Environ Sci Technol**, 50**,** pp. 8954-8976.
28. Manuel, C. M. (2007). '**Biofilm Dynamics and Drinking Water Stability: Effects of Hydrodynamics and Surface Materials**'. Ph.D Thesis, University of Porto, Portugal.
29. Manuel, C. M., Nunes, O. C. and Melo, L. F. (2007). 'Dynamics of drinking water biofilm in flow/non-flow conditions'. **Water Res**, 41**,** pp. 551-562.
30. Momba, M. N. B., Kfir, R., Venter, S. N. and Cloete, T. E. (2000). 'An overview of biofilm formation in distribution systems and its impact on the deterioration of water quality'. **Water SA**, 26**,** pp. 59-66.
31. Rusconi, R., Lecuyer, S., Guglielmini, L. and Stone, H. A. (2010). 'Laminar flow around corners triggers the formation of biofilm streamers'. **Journal of the Royal Society Interface**, 7**,** pp. 1293-1299.
32. Russ, J. C. 2011. '**The image processing handbook, Sixth Edition**', North Carolina State University, Materials Science and Engineering Department, Raleigh, North Carolina, CRC Press.
33. Saur, T., Morin, E., Habouzit, F., Bernet, N. and Escudie, R. (2017). 'Impact of wall shear stress on initial bacterial adhesion in rotating annular reactor'. **PLoS One**, 12**,** https://doi.org/10.1371/journal.pone.0172113
34. Sheng, G. P., Yu, H. Q. and Li, X. Y. (2010). 'Extracellular polymeric substances (EPS) of microbial aggregates in biological wastewater treatment systems: A review'. **Biotechnology Advances**, 28**,** pp. 882-894.
35. Simões, L. C. (2012). '**Biofilms in drinking water**'. Biofilms in drinking water: formation and control. LAMBERT Academic Publishing.
36. Son, K., Brumley, D. R. and Stocker, R. (2015). 'Live from under the lens: exploring microbial motility with dynamic imaging and microfluidics'. **Nature Reviews Microbiology**, 13**,** pp. 761-775.
37. Srinivasan, S., Harrington, G. W., Xagoraraki, I. and Goel, R. (2008). 'Factors affecting bulk to total bacteria ratio in drinking water distribution systems'. **Water Res**, 42**,** pp. 3393-3404.
38. Staudt, C., Horn, H., Hempel, D. C. and Neu, T. R. (2004). 'Volumetric measurements of bacterial cells and extracellular polymeric substance glycoconjugates in biofilms'. **Biotechnol Bioeng**, 88**,** pp. 585-592.
39. Stoodley, P., Boyle, J. D., DeBeer, D. and Lappin-Scott, H. M. (1999a). 'Evolving perspectives of biofilm structure'. **Biofouling**, 14**,** pp. 75-90.
40. Stoodley, P., Dodds, I., Boyle, J. D. and Lappin-Scott, H. M. (1999b). 'Influence of hydrodynamics and nutrients on biofilm structure'. **J Appl Microbiol**, 85**,** pp. 19S-28S.
41. Szabo, J. G., Rice, E. W. and Bishop, P. L. (2007). 'Persistence and decontamination of Bacillus atrophaeus subsp. globigii spores on corroded iron in a model drinking water system'. **Appl Environ Microbiol**, 73**,** pp. 2451-2457.
42. van Loodsdrecht, M. C. M., Eikelboom, D., Gjaltema, A., Tijhuis, L. and Heijnen, J. J. (1995). 'Biofilm structures'. **Water Science and Technology**, 32**,** pp. 35-43.

43. Wimpenny, J., Manz, W. and Szewzyk, U. (2000). 'Heterogeneity in biofilms'. **Fems Microbiology Reviews**, 24**,** pp. 661-671.
44. Yang, X. M., Beyenal, H., Harkin, G. and Lewandowski, Z. (2000). 'Quantifying biofilm structure using image analysis'. **J Microbiol Methods**, 39**,** pp. 109-119.
45. Zheng, M. Z., He, C. G. and He, Q. (2015). 'Fate of free chlorine in drinking water during distribution in premise plumbing'. **Ecotoxicology**, 24**,** pp. 2151-2155.
46. Zlatanović, Lj., van der Hoek, J. P. and Vreeburg, J. H. G. (2017). 'An experimental study on the influence of water stagnation and temperature change on water quality in a full-scale domestic drinking water system'. **Water Res**, 123, pp. 761-772.